Supplementary Results and Discussion

γTuSC Domain Architecture

The 8 Å structure provides a clear definition of domain arrangements in Spc97p and Spc98p, whose locations and orientations were inferred from our previous *in vivo* FRET and direct labelling experiments[1,2] (Supplementary Fig. 4a). The base of γTuSC, nearest the filament axis, contains the N-terminal domains of Spc97p and Spc98p, which form the primary dimerization interface between the two proteins. There is no clear demarcation between Spc97p and Spc98p in this region, where our labelling studies indicated the two proteins might be crossing over each other[1]. Extending out from the base, Spc97p and Spc98p have elongated 35-40 kDa domains; Spc98p is distinguished by a pronounced kink in this region, at a point shown to be flexible in the structure of free γTuSC (Supplementary Fig. 4a). The C-terminal 50 kDa of Spc97p and Spc98p form the γ-tubulin binding domains. It has recently been suggested that Spc97p and Spc98p may consist largely of armadillo repeats[3]. The density in the central and C-terminal domains of Spc97p has a striated pattern that may correspond to these repeats of short alpha helices (Supplementary Fig.4c).

From our labelling studies[1] we assumed a roughly linear N- to C-terminal arrangment of the three domains in Spc97p and Spc97p. The masses of the domains allow us to estimate where the domain boundaries are in each sequence (Supplementary Fig. 4b). Two conserved motifs, grip1 and grip2, are found in all of the γ-tubulin complex proteins[4]. A recent report showed that a mutation at a conserved site in the grip 1 motif of the *Arabidopsis* Spc97p homolog interfered with interactions with the Spc98p homolog[5]. This is consistent with the approximate location of grip 1 in the upper portion of the central domain, in a position where contacts are made between Spc97p and Spc98p of

adjacent γTuSCs. The grip 2 motif is within the γ-tubulin binding domain, consistent the idea that each of the γ-TuRC specific proteins may directly interact with γ-tubulin[6].

Location and role of Spc110

The location of Spc110p$^{1-220}$ is consistent with several lines of evidence. In the structure Spc110p$^{1-220}$ is associated primarily with Spc98p, with limited Spc97p contacts in the N-terminal dimerization domain. This is consistent with the observation that Spc110p interacts directly with Spc98p but only indirectly, or more weakly, with Spc97p, and that several mutations near the N-terminus of Spc97p are synthetically lethal with temperature sensitive Spc110p mutants[7]. Further, one end of the Spc110p$^{1-220}$ mass is near the center of γTuSC, where the N-terminus of Spc110p was predicted to interact based on *in vivo* FRET[2]. The other end of the presumed Spc110p$^{1-220}$ density extends beyond γTuSC and connects with disordered density closer to the helical axis (Supplementary Fig. 5b).

There are at least two ways in which Spc110p$^{1-220}$ might stabilize interactions between γTuSCs: simultaneous binding to two γTuSCs to constrain their relative mobility, or allosterically inducing subtle changes in γTuSC that promote oligomerization. The location of Spc110p$^{1-220}$ near the base of γTuSC, where the strongest inter-γTuSC contacts are made, is compatible with either mode of action.

It should be noted that extended γTuSC filaments have not been observed *in vivo*[8,9]. Full-length Spc110p, with a very long coiled-coil region, would block extension of γTuSC oligomers *in vivo*, limiting their size to a single turn. In that regard, when purified Spc110p is added to γTuSC short filaments form with Spc110p$^{1-220}$ but oligomers larger than a single ring are not observed with Spc110p$^{1-280}$, which has 60 more residues of

predicted coiled-coil (data not shown). Other factors may also limit γTuSC assembly size *in vivo*.

References

1. Choy, R.M., Kollman, J.M., Zelter, A., Davis, T.N., & Agard, D.A., Localization and orientation of the gamma-tubulin small complex components using protein tags as labels for single particle EM. J Struct Biol 168 (3), 571-574 (2009).

2. Kollman, J.M. *et al.*, The structure of the gamma-tubulin small complex: implications of its architecture and flexibility for microtubule nucleation. Mol Biol Cell 19 (1), 207-215 (2008).

3. Zizlsperger, N. & Keating, A.E., Specific coiled-coil interactions contribute to a global model of the structure of the spindle pole body. J Struct Biol.

4. Gunawardane, R.N. *et al.*, Characterization and reconstitution of Drosophila gamma-tubulin ring complex subunits. J Cell Biol 151 (7), 1513-1524 (2000).

5. Nakamura, M. & Hashimoto, T., A mutation in the Arabidopsis gamma-tubulin-containing complex causes helical growth and abnormal microtubule branching. J Cell Sci 122 (Pt 13), 2208-2217 (2009).

6. Gunawardane, R.N., Martin, O.C., & Zheng, Y., Characterization of a new gammaTuRC subunit with WD repeats. Mol Biol Cell 14 (3), 1017-1026 (2003).

7. Nguyen, T., Vinh, D.B., Crawford, D.K., & Davis, T.N., A genetic analysis of interactions with Spc110p reveals distinct functions of Spc97p and Spc98p, components of the yeast gamma-tubulin complex. Mol Biol Cell 9 (8), 2201-2216 (1998).

8. Byers, B., Shriver, K., & Goetsch, L., The role of spindle pole bodies and modified microtubule ends in the initiation of microtubule assembly in Saccharomyces cerevisiae. J Cell Sci 30, 331-352 (1978).

9. O'Toole, E.T., Winey, M., & McIntosh, J.R., High-voltage electron tomography of spindle pole bodies and early mitotic spindles in the yeast Saccharomyces cerevisiae. Mol Biol Cell 10 (6), 2017-2031 (1999).

Supplementary Movie 1. γTuSC/Spc110p filament structure. The helical reconstruction is show rotating. The front clipping plane is then brought in to show features on the filament interior, and to demonstrate the lack of connections between layers of the helix.

Supplementary Movie 2. A single ring and a single γTuSC subunit from the filament structure. A single turn of the γTuSC/Spc110p$^{1-220}$ structure coloured by subunit is shown rotating. The view is rotated to look down the helical axis to demonstrate the 13-fold γ-tubulin symmetry. A single γTuSC subunit is then shown, colored gold for γ-tubulin, dark blue for Spc98p, light blue for Spc97p, and light green for Spc110p$^{1-220}$.

Supplementary Movies 3 and 4. Reorganization of the γ-tubulin ring from the filament geometry to microtubule geometry. Initially, a single ring of thirteen γ-tubulins from the γTuSC-Spc110p$^{1-220}$ filament is shown. The γ-tubulins are then moved by linear interpolation to their corresponding positions in a microtubule lattice. Both movies show the same movement, with a view down the filament axis in Movie 3 and a perpendicular view in Movie 4.

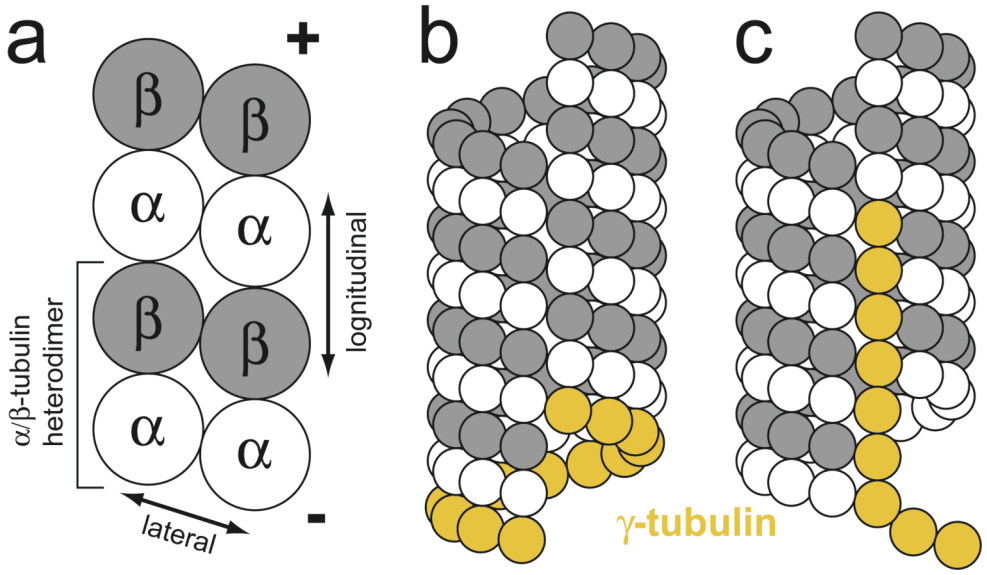

Supplementary Figure 1. Microtubule lattice contacts and possible interactions with γ-tubulin. a) α/β-tubulin heterodimers make both longitudinal and lateral contacts in the microtubule. The longitudinal contacts define protofilaments with polarity designated + and -. b) A template model for interaction with the microtubule with lateral contacts between γ-tubulins and longitudinal contacts between γ-tubulin and α-tubulin. c) A protofilament model, with longitudinal contacts between γ-tubulins and lateral contacts between γ-tubulin and α/β-tubulin.

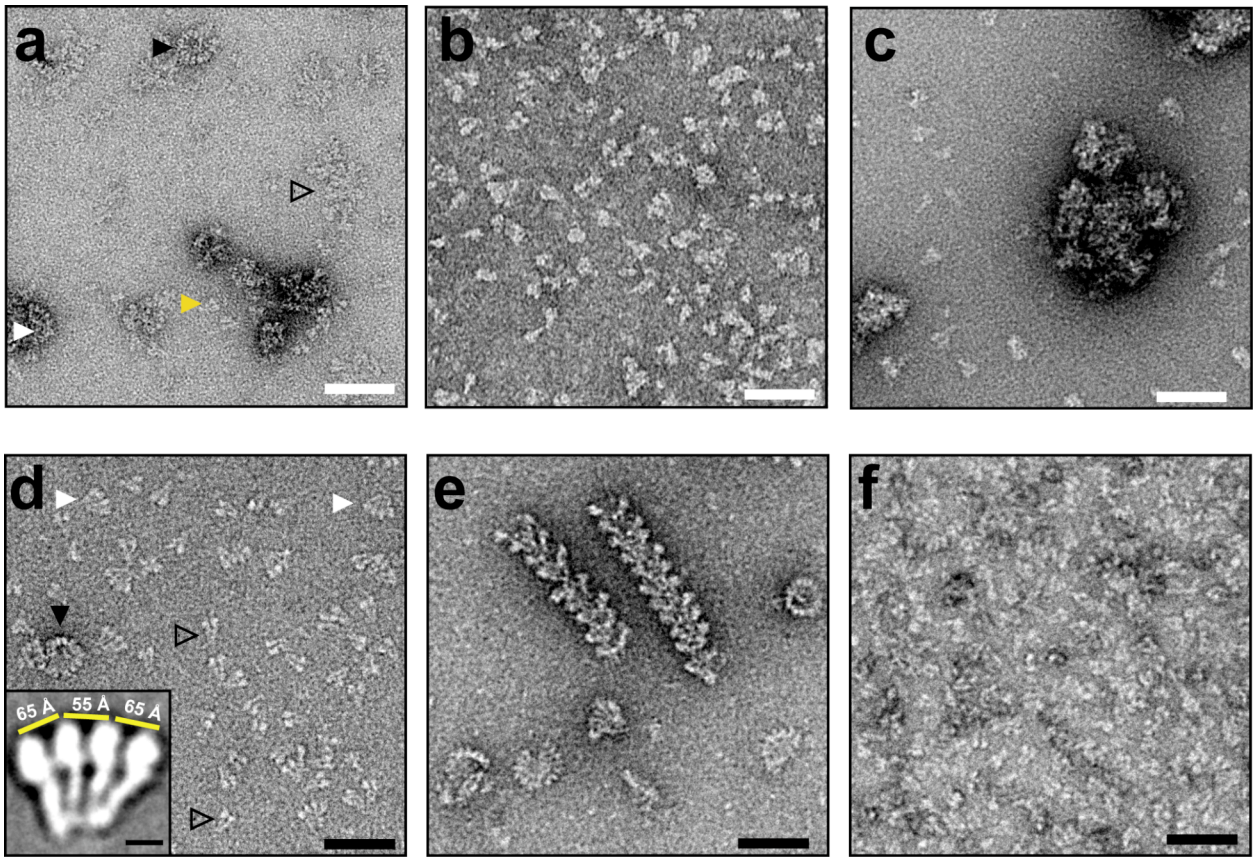

Supplementary Figure 2. Recombinant *Saccharomyces* γTuSC spontaneously assembles ring structures. a) γTuSC was diluted into BRB80 to a concentration of 0.2 μM, as in Figure 1a. Under these conditions rings (black arrows) and partial rings (white arrows) were observed, some of which were clearly flattened by the staining procedure (empty arrows). Unassembled γTuSC was also observed (yellow arrows). b) The same sample as in (a), but diluted into BRB80 + 250 mM KCl did not assemble into rings. c) The same sample as in (a) diluted into BRB80 at pH 6.2, which causes large aggregates to form. d) In negative stain micrographs of γTuSC co-purified with Spc110p$^{1-220}$ monomeric γTuSC (empty arrowheads) predominates, but many γTuSC dimers were observed (white arrowheads) and, rarely, rings (black arrowhead). Inset, average of 212 dimers, scalebar, 50 Å. The apparent distance between the centers of the inter-γTuSC γ-tubulin heads in projection is similar to the distance

seen in the structure of free γTuSC. However, it is slightly different from the actual intra-γTuSC γ-tubulin distances defined by the higher resolution EM structure (Fig. 3). e) The sample in (d), concentrated ten-fold and stabilized with glycerol. f) γTuSC alone does not form filaments under the same conditions as in (e). Scalebars, 50 nm.

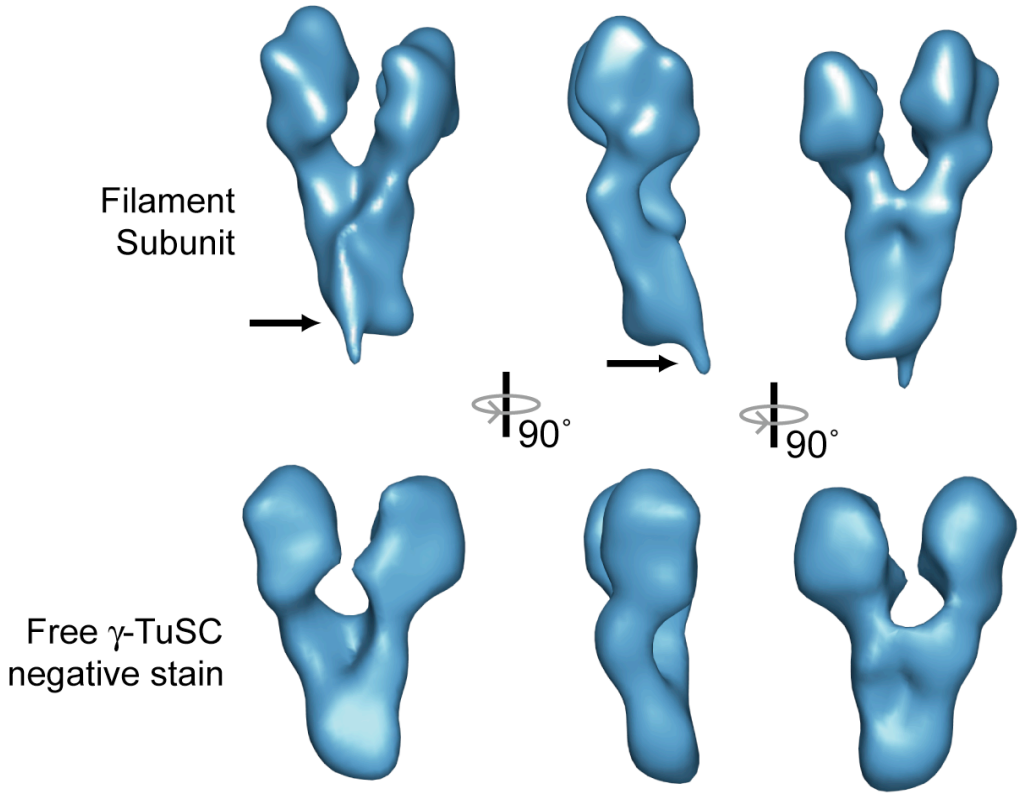

Supplementary Figure 3. Comparison of free γTuSC with the filament subunit. The negative stain reconstruction of free γTuSC (bottom) was used to identify the repeating γTuSC subunit in the filament (top). Both structures are filtered to 25 Å, the resolution of the free γTuSC structure. The primary difference between the reconstructions is the ridge of density that runs along the N-terminal third of Spc98 and extends past the base of the structure (arrows), whose occupancy varied between γTuSC preps. This density likely corresponds to part of Spc110p$^{1-220}$.

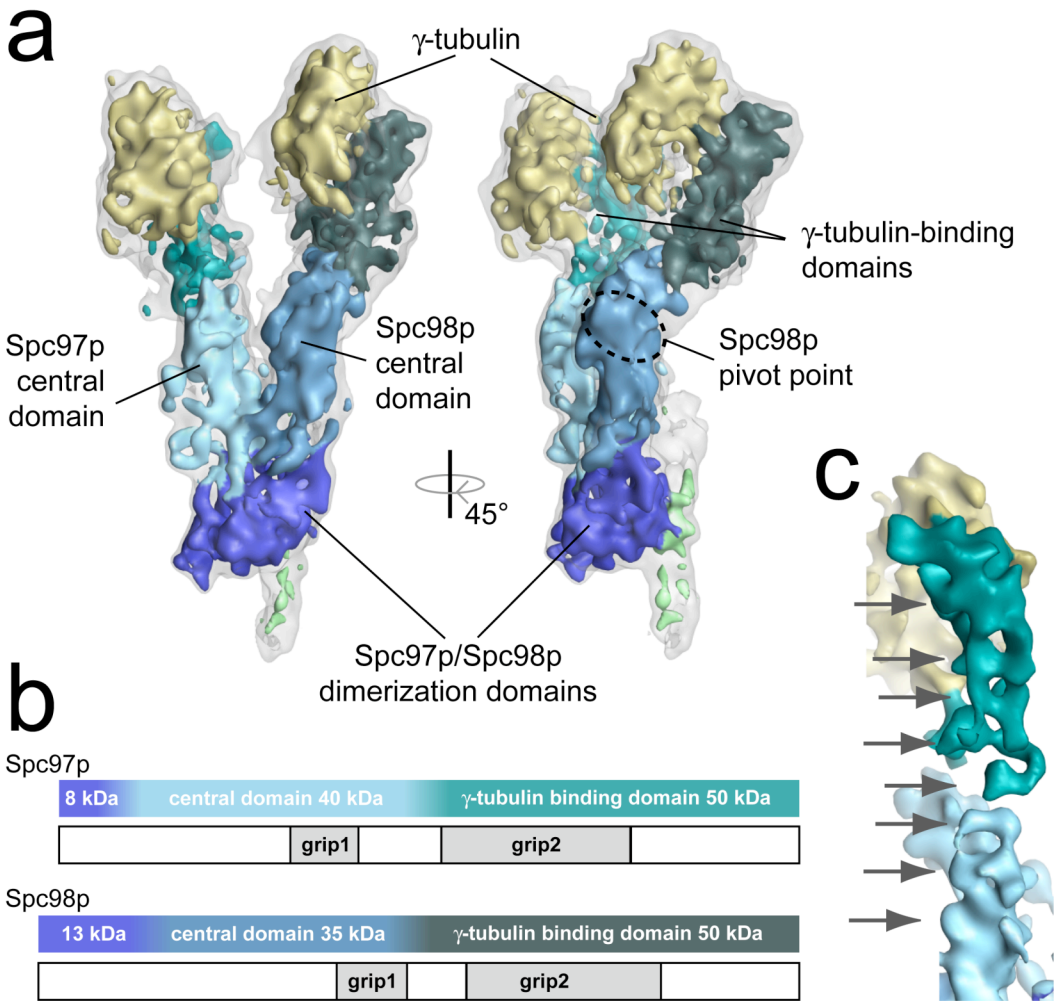

Supplementary Figure 4. Higher contour levels define the domain organization of Spc97p and Spc98p and their interfaces with γ-tubulin. a) A single γTuSC from the filament is shown as viewed from the filament interior. The contour level used in Figure 3 (transparent gray), and at a higher contour level (coloured) are shown. In the higher contour map a B factor sharpening of -500 Å^2 was applied to highlight secondary structure features. γ-tubulin, Spc97p and Spc98p were distinguished by previous labelling experiments. The segmentation of Spc97p and Spc98p into three domains is based on automated segmentation by the Segger plug-in to Chimera. The domain at the base of the structure is likely a dimerization domain between Spc97p and Spc98p, although

there is not a well-defined separation between the two proteins in this region. The approximate region of Spc98p which was shown to be flexible in our previous γTuSC negative stain reconstruction is indicated by the dashed circle. b) The approximate arrangement of Spc97p and Spc98p domains is shown, based on the assumption that the domains are arranged linearly from N- to C-terminus along the long axis of the structure. The location of the conserved grip1 and grip2 motifs is also noted. c) A close up view of the Spc97p central and C-terminal domains reveals a repeating structure (arrows), which may correspond to armadillo repeats, which have been proposed to constitute much of Spc97p and Spc98p.

a

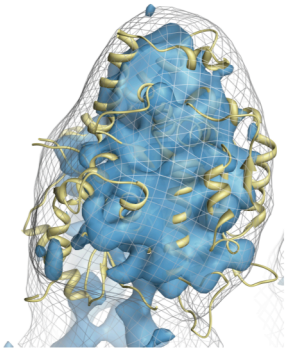

b

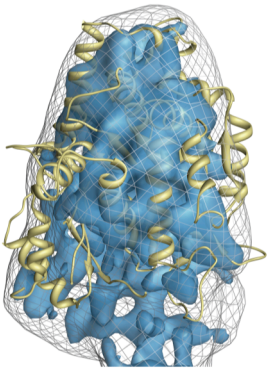

c

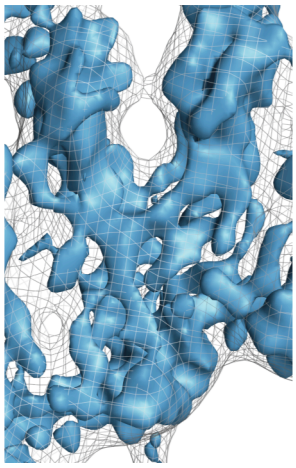

Supplementary Figure 5. The quality of the cryo-EM density map varies within the structure. a) The γ-tubulin density associated with Spc97p contoured at 1.5 σ (grey mesh) or 3.0 σ (transparent blue), with the human γ-tubulin crystal structure fit as in Figure 3. The 3.0 σ map was sharpened by application of a -500 $Å^2$ B-factor. The view is of the plus end of γ-tubulin. At higher contour levels secondary structure elements are not clearly defined, suggesting the effective resolution of this region of the EM map is somewhat lower than the 8 Å estimated for the structure as a whole. b) A view of the γ-tubulin associated with Spc98p, coloured and contoured as in (a). c) The N-terminal and central domains of Spc97p and Spc98p contoured at 1.5 σ (grey mesh) or 3.0 σ (blue). In this region tube like density, likely corresponding to alpha helices, is clearly visible, suggesting a higher resolution than in the γ-tubulin regions.

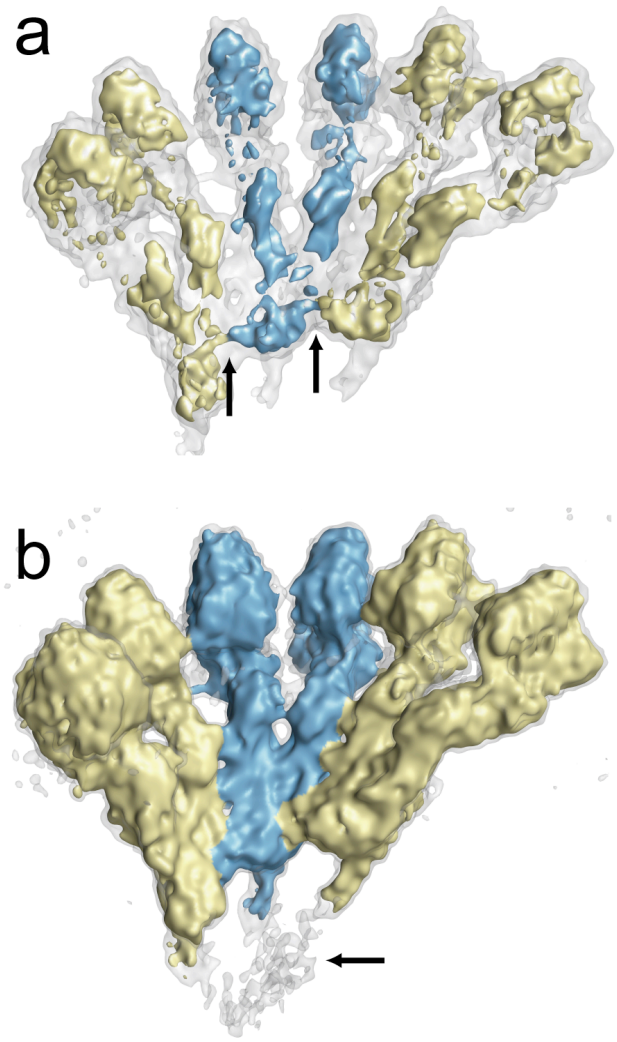

Supplementary Figure 6. Different density thresholds show strong connections between subunits at their bases, and regions of disordered density near the centre of the filament. a) Three adjacent γTuSCs are shown at the contour level used in Figure 3 (transparent gray), and a higher contour level (blue and gold) to emphasize the strong density that connects γTuSCs near their bases (arrows). b) The same map shown at the original contour (blue and gold) and a lower threshold (transparent gray) to display lower density features trailing from the the presumed Spc110p$^{1-220}$ density, in toward the center of the filament.

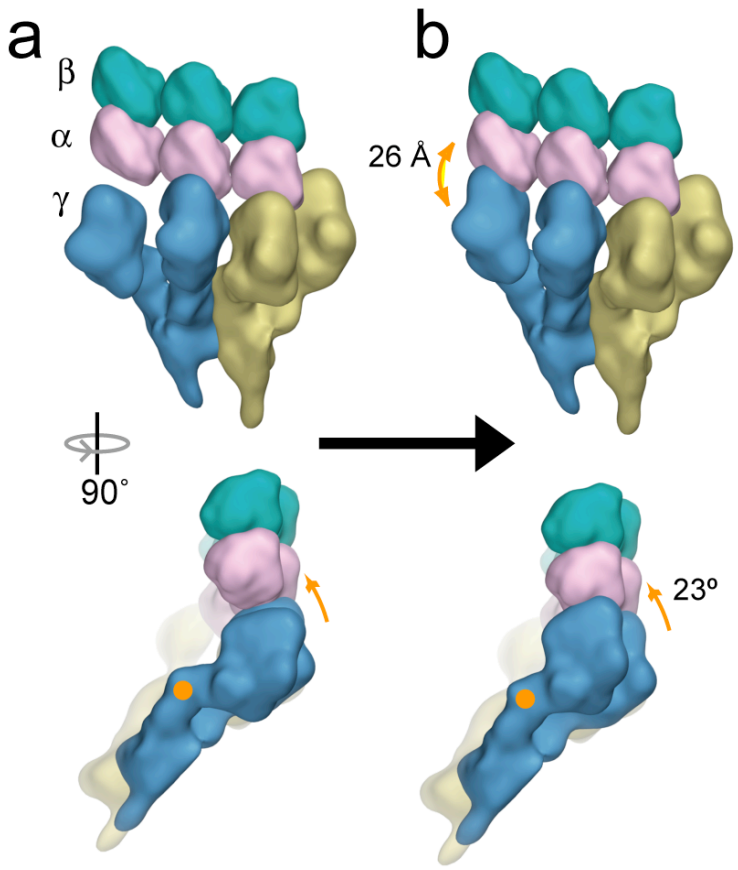

Supplementary Figure 7. Bending in the Spc98p arm would bring the intra-γTuSC γ-tubulins to the microtubule lattice spacing. a) Two adjacent γTuSCs from the filament structure (blue and gold) are aligned to α/β-tubulin from a 13-protofilament microtubule lattice so that the central γ-tubulin makes longitudinal lattice contacts with the central α-tubulin, as in Figure 4e. The mismatch between the filament γ-tubulin geometry and the microtubule geometry leaves a gap between the Spc98p-bound γ-tubulin at left and the microtubule lattice. b) A rotation at the kink in the Spc98p arm of about 26º would bring the γ-tubulin to the microtubule lattice position. The pivot point of this bending is indicated in the side views by an orange circle, and the orange arrow indicates the direction and magnitude of the γ-tubulin motion.

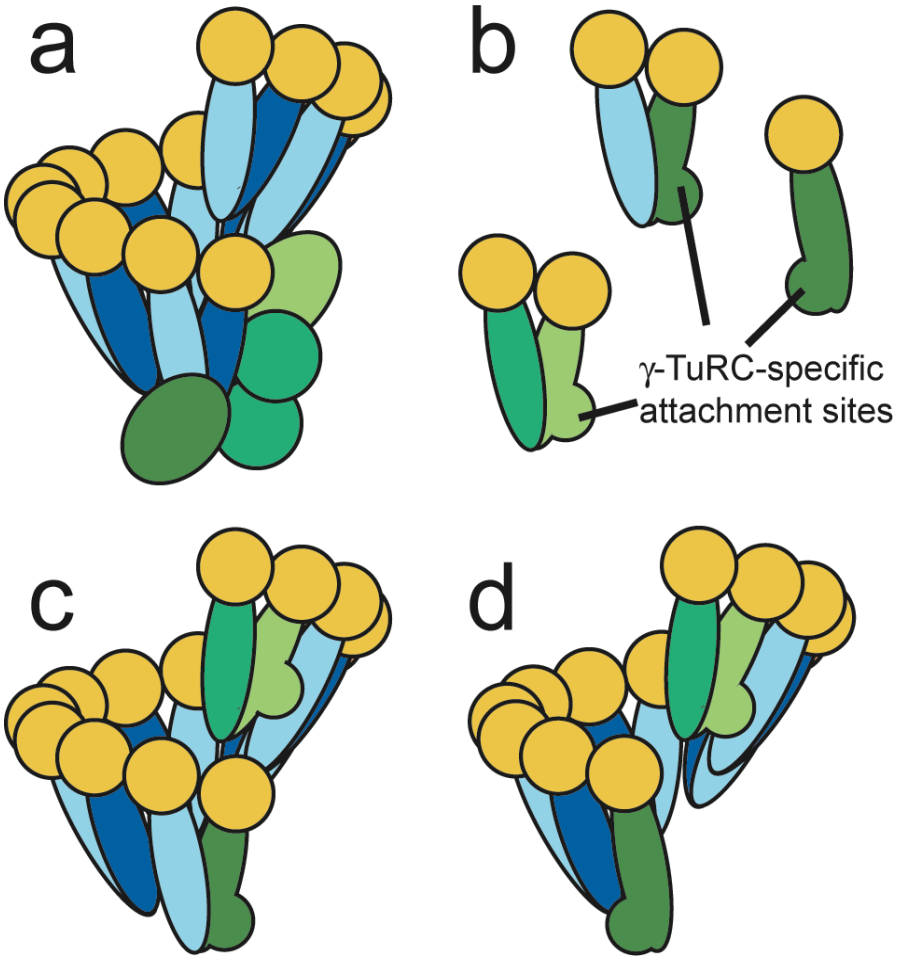

Supplementary Figure 8. Alternative models of the γ-TuRC. a) The traditional model of γ-TuRC assembly with the γ-TuRC-specific proteins (green) forming a cap structure which organizes γTuSCs (blue and gold) into a ring-like template. b) Possible alternate γTuSC-like assemblies in which the γ-TuRC-specific components replace Spc97p or Spc98p, or form a half γTuSC-like complex. c and d) Alternative models for γ-TuRC assembly in which the γ-TuRC-specific proteins form part of the ring structure, and provide unique attachment sites.